New Method for Reducing Artifactual Flow Deficits Caused by Compensation Techniques in the Choriocapillaris with Optical Coherence Tomography Angiography

Peter L. Nesper, MS, **Amani A. Fawzi, MD**

Department of Ophthalmology, Feinberg School of Medicine, Northwestern University, Chicago, Illinois

Abstract

Purpose: To mitigate artifactual choriocapillaris flow deficits in optical coherence tomography angiography (OCTA), which are a side effect of inverse structural OCT compensation.

Methods: In a modified algorithm, we set pixels in the original structural OCT that were greater than one standard deviation above the mean intensity (hyperreflective regions) to the mean pixel intensity of the image to remove hyporeflective regions in the inverse slab. We compared this algorithm to the original using flow deficit density (FDD) and multiscale structural similarity index (MS-SSIM) obtained from three distinct thresholding methods (local Phansalkar, global MinError(I) and global Li).

Results: We included 16 eyes of 16 healthy subjects (31.1 ± 6.9 years, 10 females). Using the modified OCT correction, FDD was lower compared to the original algorithm using Phansalkar ($p < 0.001$), but higher using Li thresholding ($p = 0.049$). MS-SSIM was increased after applying the modified algorithm with all three thresholding methods ($p < 0.001$), indicating a closer relationship to the original OCTA scan.

Conclusion: We demonstrate a new method that significantly reduced the introduction of artifactual flow deficits in the choriocapillaris during post-processing. Given the improved MS-SSIM, we believe our algorithm more accurately represents the choriocapillaris.

Summary Statement:

We demonstrate a new method for signal compensation in the choriocapillaris that overcomes the problem of artifactual flow deficits on optical coherence tomography angiography. The new algorithm improved similarity to the original choriocapillaris image, suggesting a more accurate representation of this vascular layer.

Corresponding author: Amani Fawzi, MD; Department of Ophthalmology, Feinberg School of Medicine, Northwestern University, 645 N. Michigan Avenue, Suite 440, Chicago, IL 60611, USA; afawzimd@gmail.com; Tel: +1 (312) 908 8152; Fax: 312-503-8152.

Introduction

The choriocapillaris is a crucial vascular layer that supplies the retinal pigment epithelium (RPE) and outer retina via diffusion from the underlying choroid. Dysfunction of the choriocapillaris is known to occur in ocular diseases, such as age-related macular degeneration, and may play an important role in the pathogenesis of neovascular age-related macular degeneration and other retinal diseases such as diabetic retinopathy.[1, 2] The advent of optical coherence tomography angiography (OCTA) led to many *in vivo* studies of the choriocapillaris.[3–6] Over time, researchers have developed methods for better visualization and improved artifact removal with the goal of accurately representing and measuring the choriocapillaris.

Zhang et al developed an approach that uses image multiplication between the original choriocapillaris OCTA and the inverted structural choriocapillaris OCT to compensate for OCT signal attenuation in the choriocapillaris due to overlying drusen and RPE changes[7], which has been widely used since.[8–12] While this technique generally performs well, Ledesma-Gil and colleagues recently reported areas of hyperreflectivity in the original structural OCT that ultimately result in new and artifactual flow deficits when using this method.[13] These authors used a similarity index between the original OCTA and the thresholded image and found that, compared to a simple threshold without compensation, the addition of the compensation method led to decreased similarity to the original image.[13] These results suggest that this commonly used method, as it is currently implemented, may not accurately represent the true choriocapillaris. The original compensation method as well as the artifactual flow deficits were reported using swept-source (SS)-OCTA, yet studies have used the compensation method in spectral-domain (SD)-OCTA as well.[10, 14, 15]

In the current study, we illustrate that the original approach introduces artifactual flow deficits when used for SD-OCTA, suggesting this issue is not limited to SS-OCTA. To overcome this, we implement a fully automated method to compensate and threshold the choriocapillaris, and compare the original algorithm to a modified approach that requires an additional step of removing hyperreflective regions in the original structural OCT. This approach was suggested as a possible solution by Ledesma-Gill et al.[13] and is similar to the method described by Camino et al.[16] who used machine learning software to detect and compensate in regions of hyporeflectivity caused by attenuated OCT signal. We report qualitative and quantitative improvements resulting from this modification implemented during inverse OCT compensation, including greater multiscale structural similarity index (MS-SSIM), and discuss the importance of this method that, we believe, more accurately represents the choriocapillaris.

Methods

This was a retrospective, cross-sectional study of healthy subjects recruited in the Department of Ophthalmology at Northwestern University in Chicago, Illinois between July 2017 and July 2018. This study protocol was approved by the Institutional Review Board of Northwestern University and adhered to the tenets of the Declaration of Helsinki. We performed this study accordance with the Health Insurance and Portability and

Accountability Act regulations. We obtained written consent from all participants prior to their participation.

Patient Criteria

We included subjects with no history of ocular disease or systemic diseases that may affect the retinal or choroidal vasculature. Only eyes with a quality index score of Q6 or greater and without large motion or shadow artifacts were included. We excluded eyes with any retinal disease, such as diabetic retinopathy, glaucoma, glaucoma suspects, and vascular occlusive diseases. We excluded eyes with high refractive error (< -6 diopters), and eyes with high grade cataracts, to minimize artifacts that may compromise OCTA image quality. We interviewed healthy subjects prior to OCTA to obtain demographic information. For those with two eligible eyes for analysis, we chose the higher quality image based on Q-score and any minor motion artifacts, if present. We also included subset of eyes with a Q-score of 10 to establish the average pixel intensity of the choriocapillaris in Q10 scans.

OCT Angiography Imaging

We obtained 3×3 mm OCTA scans centered on the fovea using the commercially available Zeiss Cirrus HD-OCT 5000–2328 (Zeiss Meditec, Inc.) with OMAG Angioplex (software version 9.5.0.8712).[17] This OCTA device has an A-scan rate of 68,000 scans per second with a light source with a central wavelength of 840 nm and a full-width at half maximum of 90 nm.[18] The 3×3 mm scanning pattern is achieved by repeating B-scan acquisition four times at each retinal position in the slow y-axis (each of the 245 total B-scans, separated by 12.5 μm) with 245 A-scans per B-scan in the fast x-axis.[19] A line scan ophthalmoscope with real-time retinal tracking is incorporated to reduce motion artifacts in this device.[20, 21] The resulting $3 \times 3 \times 2$ mm volumetric data set includes both the structural OCT data obtained from the intensity of the OCT signal as well as the registered OCTA data obtained from the phase and amplitude contrast between repeated B-scans.

Choriocapillaris image compensation and analysis

We segmented the choriocapillaris using the manufacturer's automated segmentation from 29 μm to 49 μm below the RPE. The *en face* slabs were exported as 719×719 pixel grayscale images (0–255 pixel intensity). Any errors in the automated segmentation were corrected manually using the Angioplex software. The angiographic OCTA and structural OCT of the choriocapillaris were saved and exported into FIJI,[22] a distribution of the program ImageJ. We compensated, thresholded and extracted FD parameters from the choriocapillaris image using a fully automated custom FIJI macro.[23] The OCTA image was first compensated for signal attenuation caused by shadowing artifacts or overlying pigmentary changes using the inverse structural OCT slab as previously described.[7] Specifically, compensation was implemented by multiplying the inverted and Gaussian blurred structural OCT image by the original OCTA choriocapillaris image (Figure 1). This is the step that has been shown to introduce artifact flow deficits due to hyperreflective areas in the original structural OCT image.[13] Namely, hyperreflective regions in the original structural OCT become hyporeflective regions when inverted, which, in turn, introduce new and artifactual flow deficits when multiplied by the original OCTA of the choriocapillaris (Figure 2) as previously described.[13]

The second step in the algorithm was to normalize the resulting compensated image to a quality index score of Q10, using a database of 18 eyes from 16 healthy subjects as previously described (Figure 1F, Figure 2F).[23] To normalize each image, we first obtained the average pixel intensity of the choriocapillaris OCTA from a normalizing cohort with Q-score of 10. Then, for each eye in the study cohort, we calculated a fraction representing the average choriocapillaris pixel intensity from the normalizing cohort divided by the average choriocapillaris pixel intensity from the study eye. We then multiplied each pixel in the study eye choriocapillaris image by this fraction. The third step was binarization of the choriocapillaris using three separate thresholding techniques. We used the local Phansalkar method with a pixel radius window of 5.0, which is consistent with the size of 1 to 2 inter-capillary spaces in healthy eyes.[11, 24, 25] For global thresholding, we used MinError(I) and Li. The MinError(I) method assumes a normal distribution for both the object (FD) and the background (choriocapillaris).[26, 27] Specifically, the thresholding method is based on the assumption that the frequency at which the gray level pixel intensities from 0 to 255 occur in the histogram follows a Gaussian distribution, with respect to the object (flow deficits) and the background (choriocapillaris), individually. Then, the iterative algorithm is used to find the threshold at which the object and background best fit this assumption.[26, 27] The Li thresholding method uses another iterative algorithm that determines the optimal threshold by minimizing cross entropy between the original and binarized image.[28, 29] The fourth step of the algorithm used the Max Entropy plugin to eliminate areas of any potential shadowing or projection artifacts from superficial vessels.[30] The superficial capillary plexus (SCP) vessel region segmented using Max Entropy was removed from the final binarized image before quantifying FD parameters (Figure 3J). The final step used the Analyze Particles function to quantify the total number of FD (FD count), FD density (FDD), and mean FD size (MFDS) after excluding FD under 24 μm in diameter, which is the size of 1 inter-capillary space in healthy eyes under the fovea in OCTA.[11] The denominator in FDD was adjusted for the removal of areas underlying SCP vessels in step four.

In the modified algorithm, we sought to remove artifactual flow deficits induced during the structural OCT compensation step. To do this, we first set all pixels in the original structural OCT that were greater than one standard deviation above the mean intensity (hyperreflective regions) to the mean pixel intensity of the image (Figure 3). This extra step eliminates hyporeflective regions in the inverted structural OCT, which would introduce new flow deficits during the compensation step of the OCTA. We incorporated this step into the fully automated algorithm and ran the macro using each of the same five steps as described above. In addition to FD parameters, we compared the results of the modification to the original algorithm using multiscale structural similarity index (MS-SSIM) in FIJI.[13, 31, 32] Using MS-SSIM, we assessed the similarity between the original OCTA of the choriocapillaris and each of the three binarized images, and then compared the index between iterations of the algorithm.

Statistics

All statistical analyses were performed with SPSS version 27 (IBM SPSS Statistics; IBM Corporation, Chicago, IL, USA). Shapiro Wilk tests were used to determine if data were distributed normally. Paired analyses were used to compare the original compensation

method to the modified algorithm for FD count, FDD, MFDS and MS-SSIM for each of the three thresholding techniques (Phansalkar, MinError(I) and Li). Paired-samples t tests were used for parametric data and Wilcoxon signed ranks tests were used for nonparametric data. A P-value of less than 0.05 was considered statistically significant.

Results

A total of 16 eyes from 16 healthy subjects were analyzed (age 31.1 ± 6.9 years, 10 females). Quality index scores ranged from 6–10 (mean 9.2 ± 1.2). After removing hyporeflective regions on the inverse OCT in the modified algorithm, the MS-SSIM was significantly increased in all three thresholding methods ($p < 0.001$ for all; Table 1), signifying a closer relationship to the original OCTA scan after performing the additional post-processing step. Qualitative analysis of the modified algorithm showed a reduction in apparent artifactual flow deficits, while still compensating for signal attenuation (Figure 4). While MS-SSIM was consistently improved across the three thresholding methods after applying the modified algorithm, other FD parameters were not consistent between local and global thresholding methods (Table 1). For example, with local Phansalkar thresholding FDD and MFDS were both decreased after applying the modified algorithm ($p < 0.005$ for both), while FDD and MFDS were both increased with global Li thresholding after applying the modified algorithm ($p < 0.05$ for both). With MinError(I), MFDS was increased ($p = 0.008$) and FD count was decreased ($p = 0.047$), with no difference in FDD ($p > 0.05$) after applying the modified algorithm.

Discussion

In this study, we modified a commonly used image compensation technique for visualizing the choriocapillaris and achieved a significant reduction in artifactual flow deficits compared to the original method. We found a significant improvement in the similarly between the compensated image and the original OCTA of the choriocapillaris after implementing this step, as demonstrated in healthy eyes. We believe this modification is critical to improve the algorithm's fidelity in visualizing and quantifying the choriocapillaris in OCTA.

Our modification is based on the heterogeneity of OCT signal reflectivity in the choriocapillaris (Figure 4B). In the compensation algorithm, hyporeflective regions in the structural OCT of the choriocapillaris become hyperreflective in the inverted OCT, used for compensation of the choriocapillaris OCTA. The original intent of the algorithm is to enhance flow signal compared to the original OCTA in areas underlying drusen or RPE changes.[7] Yet, as previously described,[13] hyperreflective regions in the original structural OCT become hyporeflective in the inverted structural OCT used for compensation, causing these areas to show artifactually reduced flow signal compared to the original OCTA. Ledesma-Gil and colleagues suggested segmenting and compensating only the areas of hyporeflectivity on the original OCT[13] in order to reduce the introduction of artifactual flow deficits. Compared to our algorithm, this approach would require more sophisticated image processing or machine learning algorithms to automatically detect areas of drusen and RPE changes overlying the choriocapillaris. These authors also suggested a conditional compensation technique to avoid the introduction of new flow deficits by thresholding only

the hyporeflective regions in the structural OCT while substituting the mean pixel value for the hyperreflective regions,[13] which is the approach we took in our study. This modification resets the hyperreflective pixels in the original structural OCT to the mean reflectively of the image, while leaving hyporeflective pixels unchanged. The result is improved flow signal in hyporeflective regions in the original structural OCT, as is the intention of compensation, without the introduction of new and artifactual flow deficits.

Our study used SD-OCTA, which uses a shorter wavelength resulting in less penetration into the choroid compared to SS-OCTA, where these algorithms were originally designed.[7] Yet, the utility of this compensation technique has been extended to SD-OCTA imaging studies as well.[10, 14, 15] Furthermore, the results from the current study shows that this compensation algorithm introduces similar flow deficit artifacts in SD-OCTA as were reported in SS-OCTA. Therefore, our modification of the algorithm may also be useful for SS-OCTA, but this needs to be confirmed in future studies. Further studies may also be necessary for assessing the extent to which these compensation algorithms overcompensate and introduce flow in areas where no actual flow exists. Using both SS-OCTA and SD-OCTA in the same subjects would be helpful in assessing this potential flaw.

The use of MS-SSIM is a valuable way to assess how closely the compensated and thresholded OCTA image is to the orginal.[13, 32] Its incorporation into FIJI allows quick and quantitative assessments for the similarity between two images (scale=0–1, with a greater value for more similar images). We found that MS-SSIM was significantly higher after removing hyporeflective regions on the inverse OCT using our modified algorithm in all three thresholding methods ($p < 0.001$ for all), consistent with higher fidelity to the original OCTA scan. The range for MS-SSIM in the original compensation method was 0.28–0.36 compared to 0.39–0.44 in the modified method, depending on the thresholding technique. Pairwise comparisons demonstrated higher similarity to the original OCTA scan after implementing our modified algorithm ($p < 0.001$ for all). MS-SSIM values reported in our study were similar to those previously reported in OCTA images after compensation (0.34 and 0.49).[13] Some of the values we reported were slightly lower (0.28), which could be due to our use of SD-OCTA or differences in thresholding techniques between the two studies.[13]

We used three different thresholding methods, to account for the possibility that each method can produce different results,[33] and found that the different methods were not equivalent. Phansalkar is a local method that resulted in consistently greater similarity to the original OCTA both before and after our proposed modification. Furthermore, after applying our modified algorithm, FDD and MFDS were decreased with Phansalkar, but increased with Li thresholding (Table 1). MinError(I) showed a similar increase in FDD and MFDS, but only MFDS was statistically significant ($p = 0.008$). The global thresholding methods MinError(I) and Li were chosen because the resulting thresholded images more closely resembled the original OCTA compared to other global thresholding methods. The MinError(I) method assumes a normal distribution of the object (flow deficit) and the background (choriocapillaris flow).[26, 27] The global Li thresholding method minimizes the cross-entropy between the original and the thresholded image.[28, 29] It appears that when eliminating the focal and artifactual dark regions in the compensated image, the cutoff value

Author Manuscript

for distinguishing between blood vessels and flow deficits noticeably increased. In other words, the threshold changed to a higher pixel intensity. Since this is a global thresholding method, an increase in the threshold value leads to areas that were previously counted as vessels to now be below the threshold cutoff and counted as flow deficits (Figure 4F compared to 4L, which is darker overall). This is likely the reason we found an increase in FDD and MFDS using global thresholding after implementing our modified algorithm (Table 1).

Limitations of this study were the use of only one OCTA device, which could limit the external validity of our newly implemented technique. Yet, the validity our technique can be quickly and easily assessed by researchers using other devices, or other thresholding methods. We also only studied young healthy eyes. Further analysis needs to be performed in eyes with pathologies, especially age-related macular degeneration, as well as healthy eyes in older subjects, since the reflectivity of the choriocapillaris and other ocular changes could affect the compensation algorithm. Finally, the cutoff value of 1 SD above the mean for identifying the region of hyperreflectivity was chosen empirically as it appeared to sufficiently reduce the introduction of new flow deficits while still compensating for attenuated OCT signal. Different cutoff values should be tested to identify the value that results in the most accurate representation of the choriocapillaris. This cutoff value may also be dependent on the device and software used.

In conclusion, we present a modified algorithm that mitigates artifactual flow deficits introduced by a commonly used technique for visualizing the choriocapillaris in OCTA. Using this modification, we found a significant reduction in artifactual flow deficits when compared to the original compensation method and a significant improvement in the similarly between the compensated image and the original OCTA. We believe this algorithm may have wide utility as it more accurately represents the choriocapillaris in OCTA. Additional studies are needed to confirm its generalizability to different hardware platforms (other SS- and SD-OCTA devices), as well as to eyes with pathological diagnoses.

Financial Support:

References

1. McLeod DS, Grebe R, Bhutto I, et al. Relationship between RPE and choriocapillaris in age-related macular degeneration. Invest Ophthalmol Vis Sci 2009;50:4982–4991. [PubMed: 19357355]

2. Seddon JM, McLeod DS, Bhutto IA, et al. Histopathological insights into choroidal vascular loss in clinically documented cases of age-related macular degeneration. JAMA Ophthalmol 2016;134:1272–1280. [PubMed: 27657855]

3. Choi W, Mohler KJ, Potsaid B, et al. Choriocapillaris and choroidal microvasculature imaging with ultrahigh speed OCT angiography. PloS one 2013;8:e81499. [PubMed: 24349078]

4. Jia Y, Bailey ST, Wilson DJ, et al. Quantitative optical coherence tomography angiography of choroidal neovascularization in age-related macular degeneration. Ophthalmology 2014;121:1435–1444. [PubMed: 24679442]

5. Moult EM, Alibhai AY, Rebhun C, et al. Spatial distribution of choriocapillaris impairment in eyes with choroidal neovascularization secondary to age-related macular degeneration: a quantitative OCT angiography study. Retina 2020;40:428–445. [PubMed: 31415449]

6. Borrelli E, Uji A, Sarraf D, Sadda SR. Alterations in the choriocapillaris in intermediate age-related macular degeneration. Invest Ophthalmol Vis Sci 2017;58:4792–4798. [PubMed: 28973325]

7. Zhang Q, Zheng F, Motulsky EH, et al. A novel strategy for quantifying choriocapillaris flow voids using swept-source OCT angiography. Invest Ophthalmol Vis Sci 2018;59:203–211. [PubMed: 29340648]

8. Borrelli E, Shi Y, Uji A, et al. Topographic analysis of the choriocapillaris in intermediate age-related macular degeneration. Am J Ophthalmol 2018;196:34–43. [PubMed: 30118688]

9. Zheng F, Zhang Q, Shi Y, et al. Age-dependent changes in the macular choriocapillaris of normal eyes imaged with swept-source optical coherence tomography angiography. Am J Ophthalmol 2019;200:110–122. [PubMed: 30639367]

10. Tiosano L, Byon I, Alagorie AR, et al. Choriocapillaris flow deficit associated with intraretinal hyperreflective foci in intermediate age-related macular degeneration. Graefes Arch Clin Exp Ophthalmol 2020;258:2353–2362. [PubMed: 32666252]

11. Chu Z, Cheng Y, Zhang Q, et al. Quantification of Choriocapillaris with Phansalkar local Thresholding: pitfalls to avoid. Am J Ophthalmol 2020;213:161–176. [PubMed: 32059979]

12. Shi Y, Chu Z, Wang L, et al. Validation of a compensation strategy used to detect choriocapillaris flow deficits under drusen with swept source OCT angiography. Am J Ophthalmol 2020;220:115–127. [PubMed: 32621895]

13. Ledesma-Gil G, Fernandez-Avellaneda P, Spaide RF. Swept-source optical coherence tomography angiography image compensation of the choriocapillaris induces artifacts. Retina 2020;40:1865–1872. [PubMed: 32453067]

14. Nassisi M, Baghdasaryan E, Borrelli E, et al. Choriocapillaris flow impairment surrounding geographic atrophy correlates with disease progression. PLoS One 2019;14:e0212563. [PubMed: 30794627]

15. Scharf JM, Corradetti G, Alagorie AR, et al. Choriocapillaris Flow Deficits and Treatment-Naïve Macular Neovascularization Secondary to Age-Related Macular Degeneration. Invest Ophthalmol Vis Sci 2020;61:11–11.

16. Camino A, Guo Y, You Q, et al. Detecting and measuring areas of choriocapillaris low perfusion in intermediate, non-neovascular age-related macular degeneration. Neurophotonics 2019;6:041108. [PubMed: 31528658]

17. Wang RK, An L, Francis P, Wilson DJ. Depth-resolved imaging of capillary networks in retina and choroid using ultrahigh sensitive optical microangiography. Optics letters 2010;35:1467–1469. [PubMed: 20436605]

18. An L, Shen T, Wang RK. Using ultrahigh sensitive optical microangiography to achieve comprehensive depth resolved microvasculature mapping for human retina. Journal of biomedical optics 2011;16:106013. [PubMed: 22029360]

19. Rosenfeld PJ, Durbin MK, Roisman L, et al. ZEISS Angioplex™ spectral domain optical coherence tomography angiography: technical aspects. OCT angiography in retinal and macular diseases 2016;56:18–29.

20. Zhang Q, Lee CS, Chao J, et al. Wide-field optical coherence tomography based microangiography for retinal imaging. Scientific reports 2016;6:1–10. [PubMed: 28442746]

21. Zhang Q, Huang Y, Zhang T, et al. Wide-field imaging of retinal vasculature using optical coherence tomography-based microangiography provided by motion tracking. Journal of biomedical optics 2015;20:066008. [PubMed: 26102573]

22. Schindelin J, Arganda-Carreras I, Frise E, et al. Fiji: an open-source platform for biological-image analysis. Nat Methods 2012;9:676–682. [PubMed: 22743772]

23. Nesper PL, Ong JX, Fawzi AA. Exploring the relationship between multi-layered choroidal neovascularization and choriocapillaris flow deficits in age-related macular degeneration. Invest Ophthalmol Vis Sci 2021;62:12–12.

24. Chu Z, Zhang Q, Gregori G, et al. Guidelines for imaging the choriocapillaris using OCT angiography. Am J Ophthalmol 2020;222:92–101. [PubMed: 32891694]

25. Phansalkar N, More S, Sabale A, Joshi M. Adaptive local thresholding for detection of nuclei in diversity stained cytology images. Int Conf Signal Process Commun: IEEE; 2011:218–220.

26. Kittler J, Illingworth J. Minimum error thresholding. Pattern Recognit 1986;19:41–47.

27. Cho S, Haralick R, Yi S. Improvement of Kittler and Illingworth's minimum error thresholding. Pattern Recognit 1989;22:609–617.

28. Li CH, Lee C. Minimum cross entropy thresholding. Pattern Recognit 1993;26:617–625.

29. Li C, Tam PK-S. An iterative algorithm for minimum cross entropy thresholding. Pattern Recognit Lett 1998;19:771–776.

30. Pun T A new method for grey-level picture thresholding using the entropy of the histogram. Signal Processing 1980;2:223–237.

31. Wang Z, Bovik AC, Sheikh HR, Simoncelli EP. Image quality assessment: from error visibility to structural similarity. IEEE Trans Image Process 2004;13:600–612. [PubMed: 15376593]

32. Renieblas GP, Nogués AT, González AM, et al. Structural similarity index family for image quality assessment in radiological images. J Med Imaging 2017;4:035501.

33. Mehta N, Liu K, Alibhai AY, et al. Impact of binarization thresholding and brightness/contrast adjustment methodology on optical coherence tomography angiography image quantification. Am J Ophthalmol 2019;205:54–65. [PubMed: 30885708]
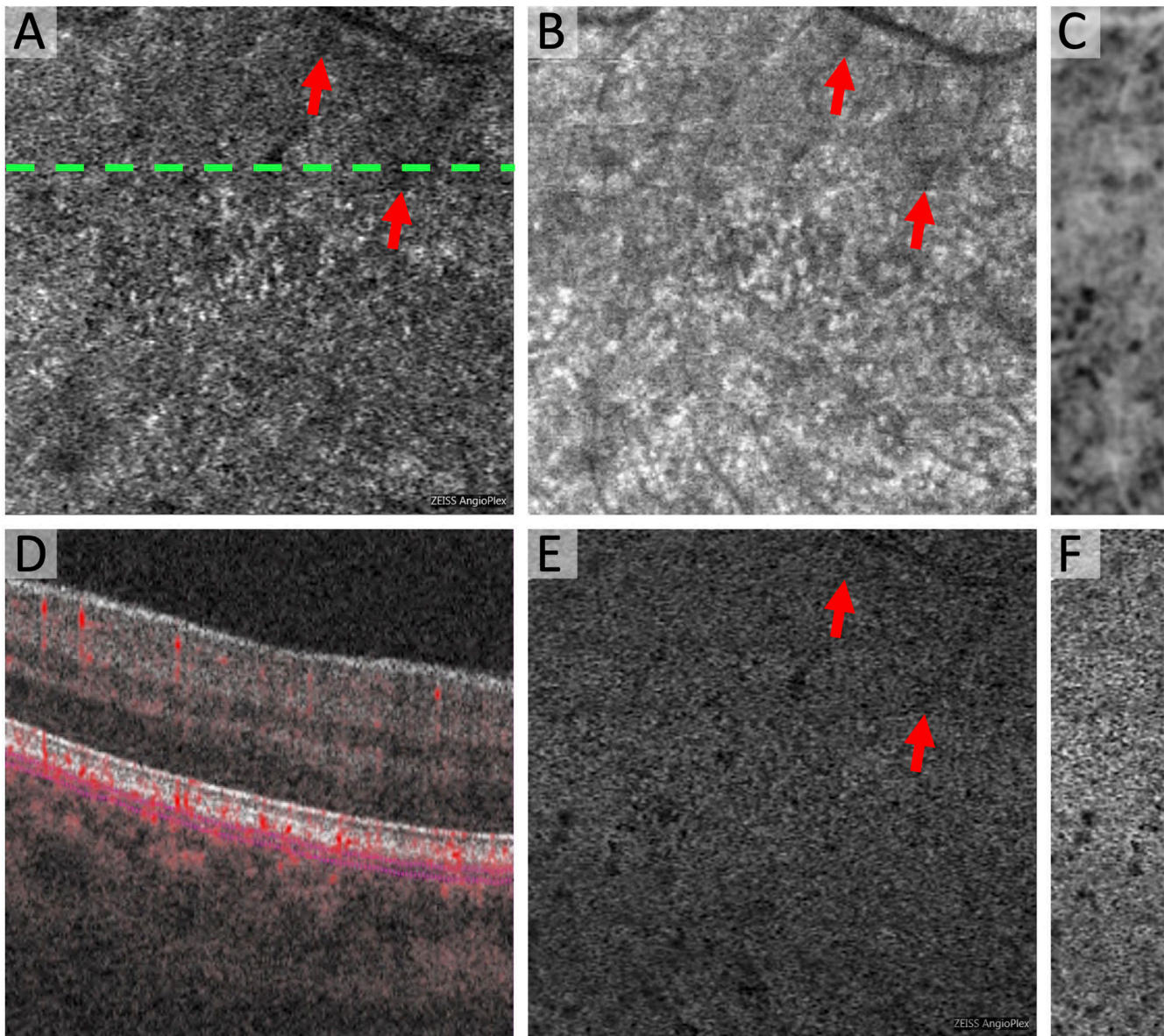
Figure 1. Original Method for Compensation for Signal Attenuation in the Choriocapillaris.
(A) Original Zeiss Angioplex OCTA of the choriocapillaris with dotted line showing location of OCTA B-scan in (D). (B) Original structural OCT of the choriocapillaris with same segmentation as (A). Arrows point to hyporeflective regions. (C) Inverted and blurred structural OCT. Shadow region is now hyperreflective. (E) Compensated OCTA as a result of multiplication of (A) x (C). (F) Final OCTA image with global compensation for Q-score. The areas of shadowing are no longer areas of flow deficit as seen in the original choriocapillaris (A).
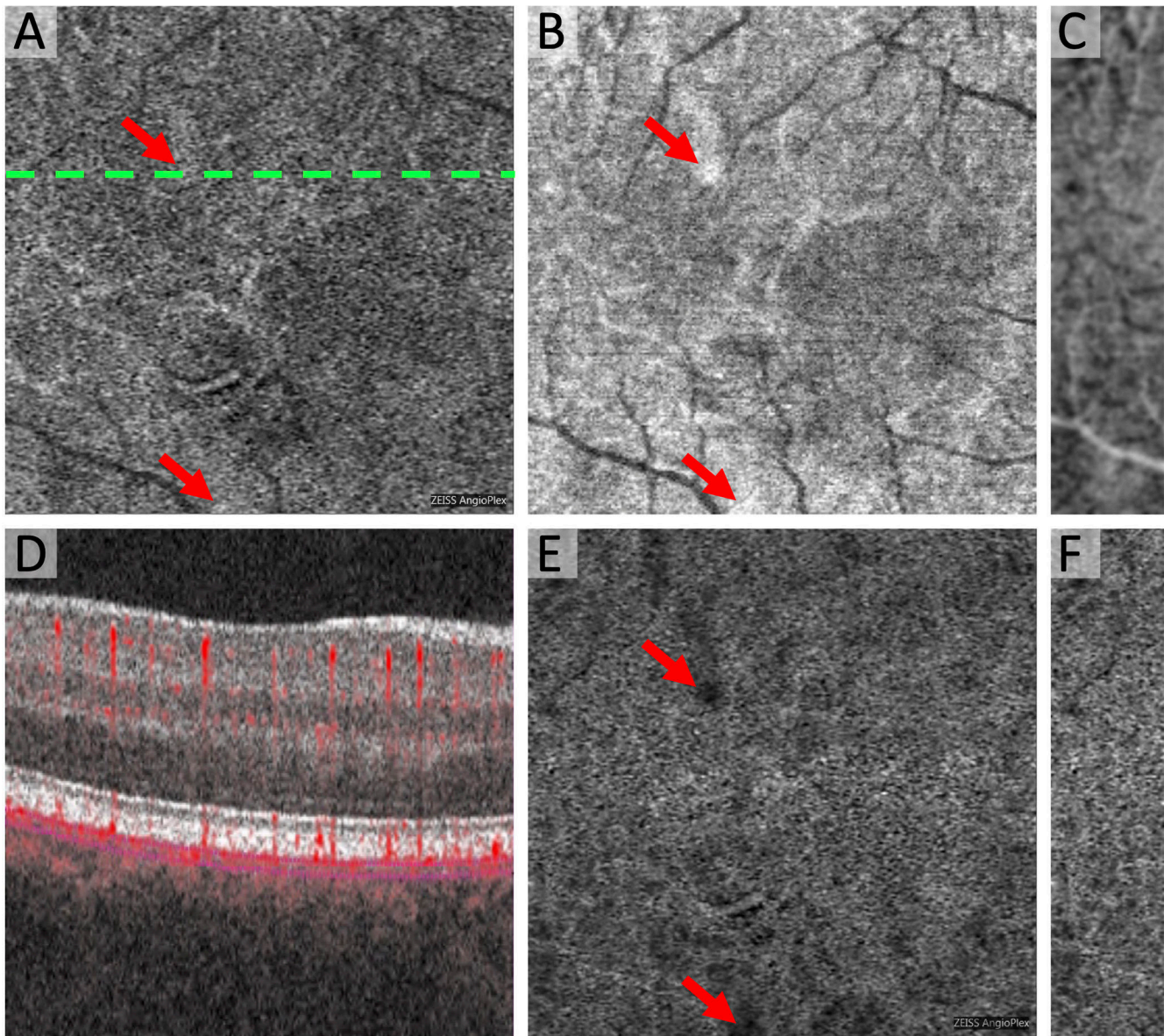
Figure 2. Compensation for Signal Attenuation Introduces Artifactual Flow Deficits in the Choriocapillaris.
(A) Original Zeiss Angioplex OCTA of the choriocapillaris with dotted line showing location of OCTA B-scan in (D). (B) Original structural OCT of the choriocapillaris with same segmentation as (A) and areas of hyperreflectivity (arrows). (C) Inverted and blurred structural OCT now with areas of relative hyporeflectivity (arrows). (E) Compensated OCTA as a result of multiplication of (A) x (C). (F) Final OCTA image with global compensation for Q-score showing newly introduced flow deficits that are not present in the original OCTA (A). These artifacts are related to the hyporeflective areas in the inverted structural OCT (arrows in C).
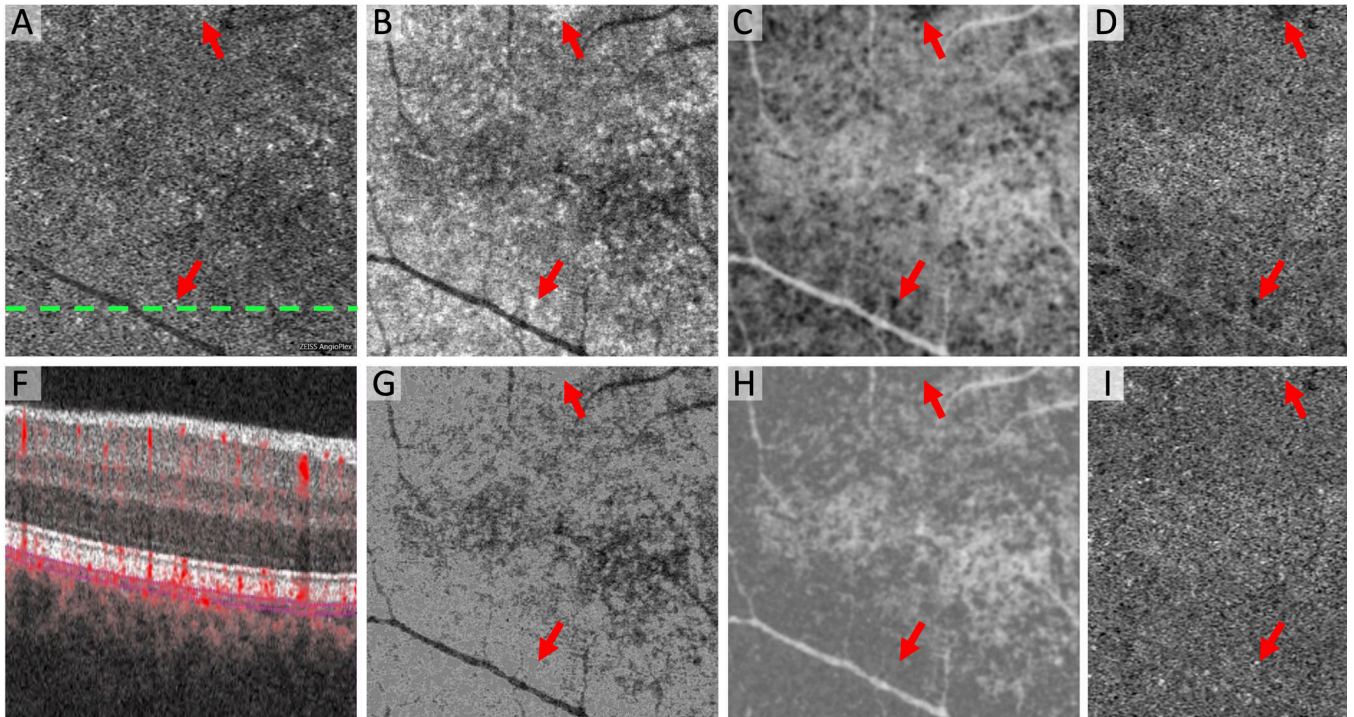
Figure 3. New Method for Reducing Artifactual Flow Deficits Caused by OCT Compensation in the Choriocapillaris.

(A) Original Zeiss Angioplex OCTA of the choriocapillaris with dotted line showing location of OCTA B-scan in (F). (B) Original structural OCT of the choriocapillaris with same segmentation as (A) and areas of hyperreflectivity (arrows). (C) Inverted and blurred structural OCT now with areas of hyporeflectivity (arrows). (D) Compensated OCTA as a result of multiplication of (A) x (C) showing new flow deficits (arrows). (E) Original OCTA of the superficial capillary plexus. (G) Structural OCT of the choriocapillaris using the modified algorithm that removes hyperreflective areas (arrows). (H) Inverted and blurred structural OCT without hyporeflective areas (arrows). (I) Compensated OCTA as a result of multiplication of (A) x (H) using the modified algorithm, which reduces artifactual flow deficits (arrows). (J) Vessel segmentation of the superficial capillary plexus using Max Entropy plugin. White regions (vessels) were removed from the final binarized images before quantifying flow deficits.
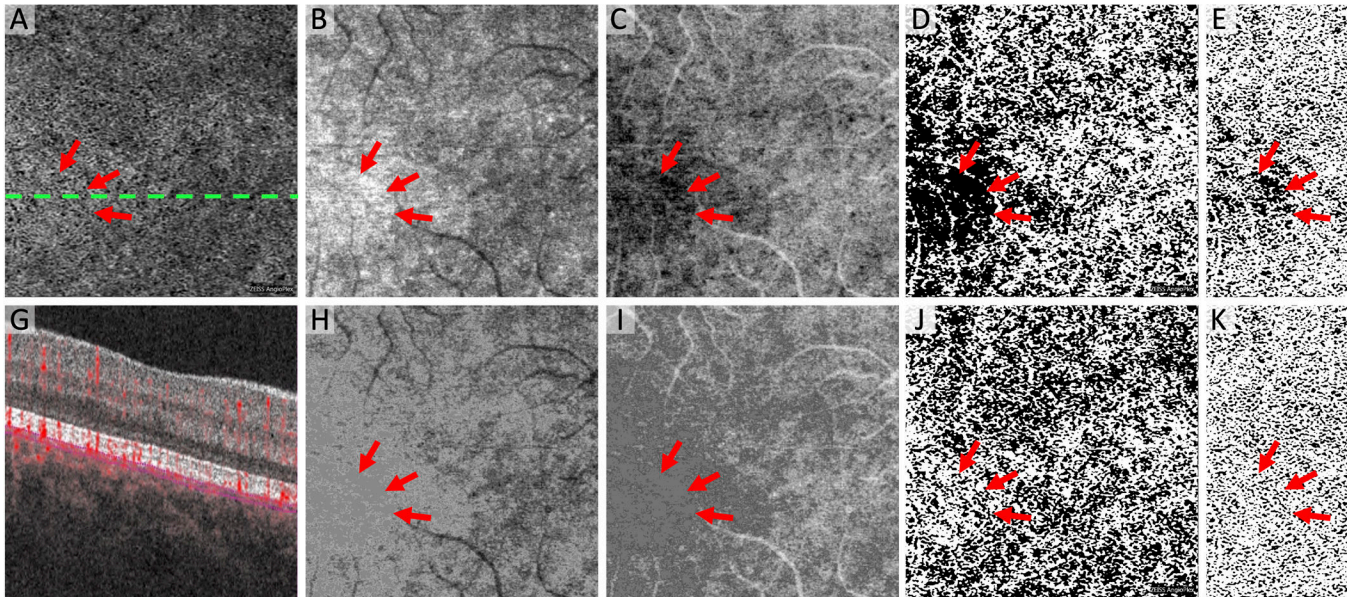
Figure 4. Modified Approach Reduces of Artifactual Flow Deficits Caused by Image Compensation.

(A) Original Zeiss Angioplex choriocapillaris OCTA flow image with dotted line indicating location of cross-section below showing segmentation lines (G). (B and H) Choriocapillaris structural OCT images. (C and I) Inverse of the structural OCT used to compensate for signal attenuation. Note inverted slab is Gaussian blurred before multiplication with OCTA. (D and J) MinError(I), (E and K) Phansalkar, and (F and L) Li thresholded images after compensation. Bottom row uses the modified algorithm for eliminating hyporeflective regions in the inverse OCT and the top row does not, which leads to large new flow deficits (arrows).

Table 1.

Differences in flow deficit measurements between the original and modified signal compensation algorithm in healthy subjects

Thresholding Method	Parameter	Original Mean ± SD	Modified Mean ± SD	P-value
Phansalkar	FD Count	938 ± 146	947 ± 190	0.709
	MFDS (μm^2)(†)	1565 ± 467	1272 ± 252	0.001*
	FDD	0.18 ± 0.06	0.15 ± 0.06	<0.001*
MinError(I)	FD Count (†)	361 ± 77	350 ± 47	0.047*
	MFDS (μm^2)(†)	10319 ± 2757	12152 ± 2149	0.008*
	FDD (†)	0.47 ± 0.12	0.51 ± 0.01	0.215
Li	FD Count	401 ± 79	365 ± 84	0.025*
	MFDS (μm^2)(†)	10575 ± 4000	12360 ± 5537	0.011*
	FDD	0.49 ± 0.04	0.50 ± 0.03	0.049*
Phansalkar	MS-SSIM	0.36 ± 0.04	0.44 ± 0.02	<0.001*
MinError(I)	MS-SSIM	0.28 ± 0.06	0.39 ± 0.03	<0.001*
Li	MS-SSIM	0.28 ± 0.06	0.39 ± 0.03	<0.001*

Flow deficit and similarity indices before (original) and after (modified) removing hyporeflective regions in the inverted OCT were compared using pairwise analyses. All statistical tests for *P*-value column were parametric two-tailed paired samples t-tests, except those labelled (†) for nonparametric Wilcoxon signed ranks test. FD = flow deficit, FDD = flow deficit density, MFDS = mean flow deficit size, MS-SSIM = multiscale structural similarity index, SD = standard deviation. Asterisks indicate statistical significance (*P*-value of less than 0.05).